Journal of Nuclear Medicine, published on October 4, 2019 as doi:10.2967/jnumed.119.233122

Theranostics targeting fibroblast activation protein in the tumor stroma: ^{64}Cu- and ^{225}Ac-labelled FAPI-04 in pancreatic cancer xenograft mouse models

Tadashi Watabe[1,2]; Yuwei Liu[1]; Kazuko Kaneda-Nakashima[2,3]; Yoshifumi Shirakami[2]; Thomas Lindner[4]; Kazuhiro Ooe[1,2]; Atsushi Toyoshima[2]; Kojiro Nagata[5]; Eku Shimosegawa[2,6]; Uwe Haberkorn[4,7,8]; Clemens Kratochwil[4], Atsushi Shinohara[2,9], Frederik Giesel[2,4], Jun Hatazawa[2,10]

Department of Nuclear Medicine and Tracer Kinetics, Graduate School of Medicine, Osaka University [1]

Institute for Radiation Sciences, Osaka University [2]

Core for Medicine and Science Collaborative Research and Education, Project Research Center for Fundamental Sciences, Graduate School of Science, Osaka University [3]

Department of Nuclear Medicine, University Hospital Heidelberg, Heidelberg, Germany [4]

Radioisotope Research Center, Institute for Radiation Sciences, Osaka University [5]

Department of Molecular Imaging in Medicine, Graduate School of Medicine, Osaka University [6]

Clinical Cooperation Unit Nuclear Medicine DKFZ, Heidelberg, Germany[7]

Translational Lung Research Center Heidelberg (TLRC), German Center for Lung Research (DZL), Heidelberg, Germany[8]

Department of Chemistry, Graduate School of Science, Osaka University [9]

Research Center for Nuclear Physics, Osaka University [10]

Corresponding and first author:

Tadashi Watabe (Assistant Professor)

2-2 Yamadaoka, Suita, Osaka 565-0871 JAPAN

TEL: +81-6-6879-3461 FAX: +81-6-6879-3469

E-Mail: watabe@tracer.med.osaka-u.ac.jp

Total word count: 4,982 words

Short running title: Theranostics targeting FAP

ABSTRACT

Fibroblast activation protein (FAP), which promotes tumor growth and progression, is overexpressed in cancer-associated fibroblasts of many human epithelial cancers. Owing to its low expression in normal organs, FAP is an excellent target for theranostics. In this study, we used radionuclides with relatively long half-lives, ^{64}Cu (half-life = 12.7 h) and ^{225}Ac (half-life = 10 days), to label FAP inhibitors (FAPI) in mice with human pancreatic cancer xenografts.

Methods: Male nude mice (body weight = 22.5 ± 1.2 g) were subcutaneously injected with human pancreatic cancer cells (PANC-1, n = 12; MIA PaCa-2, n = 8). Tumor xenograft mice were investigated after the intravenous injection of ^{64}Cu-FAPI-04 (7.21 ± 0.46 MBq) by dynamic and delayed PET scans (2.5 h post injection). Static scans 1 h after the injection of ^{68}Ga-FAPI-04 (3.6 ± 1.4 MBq) were also acquired for comparisons using the same cohort of mice (n = 8).

Immunohistochemical staining was performed to confirm FAP expression in tumor xenografts using an FAP-alpha antibody. For radioligand therapy, ^{225}Ac-FAPI-04 (34 kBq) was injected into PANC-1 xenograft mice (n = 6). Tumor size was monitored and compared to that of control mice (n = 6).

Results: Dynamic imaging of ^{64}Cu-FAPI-04 showed rapid clearance through the kidneys and slow washout from tumors. Delayed PET imaging of ^{64}Cu-FAPI-04 showed mild uptake in tumors and relatively high uptake in the liver and intestine. Accumulation levels in the tumor or normal organs were significantly higher for ^{64}Cu-FAPI-04 than ^{68}Ga-FAPI-04, except in the heart, and excretion in the urine was higher for ^{68}Ga-FAPI-04 than ^{64}Cu-FAPI-04. Immunohistochemical staining revealed abundant FAP expression in the stroma of xenografts. ^{225}Ac-FAPI-04 injection showed significant tumor growth suppression in the PANC-1 xenograft mice compared to the control mice, without a significant change in body weight.

Conclusion: This proof of concept study showed that ^{64}Cu-FAPI-04 and ^{225}Ac-FAPI-04 could be used in theranostics for the treatment of FAP-expressing pancreatic cancer. Alpha therapy targeting FAP in the cancer stroma is effective and will contribute to the development of a new treatment strategy.

Keywords: theranostics, fibroblast activation protein, pancreatic cancer, alpha therapy, actinium

INTRODUCTION

In targeted alpha therapy and theranostics, cancer-specific biomarkers, such as prostate-specific membrane antigen (PSMA) for prostate cancer (*1,2*), have limited expression in other cancer types and therefore are not generalizable for the development of a universal cancer therapy. The tumor microenvironment (stroma), which consists of non-malignant cells such as macrophages, fibroblast, endothelial cells and others, appears as a novel and promising target. In the stroma, cancer-associated fibroblasts are crucial components which stimulate cancer cell growth and invasion (*3-5*). Fibroblast activation protein (FAP), which promotes tumor growth and progression, is overexpressed in cancer-associated fibroblasts of many human epithelial cancers (*6*). FAP expression is also correlated with prognosis (*7*). Since it is expressed at low levels in normal tissues, FAP is an excellent target for theranostics in oncology. Recently, small molecule FAP inhibitor (FAPI) probes were developed (*8-10*), and the diagnostic utility of

^{68}Ga-FAPI PET has been established in various cancer types, demonstrating rapid distribution at the target site and minimal uptake in normal organs (*11,12*). In addition, Loktev et al. successfully increased FAP binding and improved pharmacokinetics by the chemical modification of the FAPI probes (*10*). They also reported high uptake of ^{177}Lu-labeled FAPI derivatives in HT-1080-FAP tumor-bearing mice. However, the efficacy of alpha emitters targeting FAP remains unknown. In this study, we used radionuclides with longer half-lives, ^{64}Cu (half-life = 12.7 h) and ^{225}Ac (half-life = 10 days), for the labelling of FAPI for evaluations of tumor uptake in the delayed phase after injection. The purpose of this study was to evaluate the biodistribution and treatment effect of ^{225}Ac-labeled and ^{64}Cu-labeled FAPI in FAP-positive human pancreatic cancer xenografts.

MATERIALS AND METHODS

Preparation of ^{64}Cu-, ^{68}Ga-, and ^{225}Ac-labeled FAPI-04 Solutions

The FAPI-04 precursor was obtained from Heidelberg University based on a material transfer agreement for collaborative research. $^{64}CuCl_2$ dissolved in 0.1 mol/L hydrochloride was purchased from Fuji Film Toyama Chemicals (Tokyo, Japan). In a micro tube, the $^{64}CuCl_2$ solution (74 MBq, 0.035 mL), 0.2 mol/L ammonium acetate (0.47 mL), 2% sodium ascorbate (0.5 mL), and 1 mmol/L FAP-04 (0.028 mL) were added and reacted at 80°C for 1 h. A ^{68}Ge-^{68}Ga generator was purchased from iTG Isotope Technologies Garching GmbH (Garching, Germany). ^{68}Ga was eluted with a solution of 0.1 mol/L hydrochloride from the generator. In a micro tube, the ^{68}Ga solution (64MBq), 2.5 mol/L sodium acetate (0.03 mL), 10% ascorbic acid (0.02 mL), and 1 mmol/L FAPI-04 (0.03 mL) were added and reacted at 95°C for 20 min.

^{225}Ac was obtained by milking from its grandparent nuclide ^{229}Th via ^{225}Ra (*13*). A dry residue containing ^{229}Th and its descendant nuclides was dissolved with 8 mol/L HNO_3 (0.5 mL) and was loaded on 2 connected anion-exchange columns (Muromac

1 × 8, 100–200 mesh, NO_3^- form, ~1-mL column volume). Then, 8 mol/L HNO_3 (3 mL) was loaded onto the columns to elute ^{225}Ra and ^{225}Ac. For only the bottom column, 8 mol/L HNO_3 (3 mL) was additionally loaded to completely strip ^{225}Ra and ^{225}Ac. ^{229}Th on the top column was separately recovered with 2 mol/L HCl (10 mL) and distilled water (5 mL). The 8 mol/L HNO_3 effluent was diluted to 4 mol/L HNO_3 and loaded on a column filled with DGA branched resin (2-mL cartridge; Eichrom, Lisle, IL, USA). After ^{225}Ra was eluted with 4 mol/L HNO_3 (6 mL), ^{225}Ac was stripped with 0.05 M HNO_3 (10 mL). After evaporation to dryness, ^{225}Ac was dissolved in a 0.2 mol/L ammonium acetate solution (0.2 mL). The radioactivity of ^{225}Ac was determined from the γ-ray emissions for ^{221}Fr (218keV) and ^{213}Bi (440keV), which were in radioactive secular equilibrium with its parent ^{225}Ac, using a high-purity germanium detector (BE-2020; Canberra, Meriden, CT, USA). In a micro tube, the ^{225}Ac solution (130 kBq, 0.2 mL), 0.2 mol/L ammonium acetate (0.1

mL), 7% sodium ascorbate (0.1 mL), and 1 mmol/L FAPI-04 (0.3 mL) were added and reacted at 80°C for 2 h.

Radiochemical yields for the three products labelled with ^{64}Cu, ^{68}Ga, and ^{225}Ac were analyzed by cellulose acetate electrophoresis. An aliquot of each product was spotted on a strip of cellulose acetate. The voltage applied to the strip was 133 V at 1 mA/cm in a solution of 0.06 mol/L barbital buffer (pH 8.6) for 40 min. The strip was exposed to an imaging plate and the radioactivity on the strip was analyzed using a bioimager (Typhoon7000; GE Healthcare, Chicago, IL, USA). The radiochemical yields of ^{64}Cu-FAPI-04, ^{68}Ga-FAPI-04, and ^{225}Ac-FAPI-04 were 85.0–88.5%, 95.0%, and 94.7–96.9%, respectively.

Preparation of Xenograft Models

PANC-1 and MIA PaCa-2 cells were obtained from American Type Culture Collection (ATCC) (Manassas, VA, USA). The cells were maintained in culture medium (RPMI1640 with L-glutamine and Phenol Red (FUJIFILM Wako Pure

Chemical, Osaka, Japan) for PANC-1 and D-MEM (High Glucose) with L-glutamine and Phenol Red (FUJIFILM Wako Pure Chemical) for MIA PaCa-2) with 10% heat-inactivated fetal bovine serum and 1% penicillin-streptomycin. Male nude mice were purchased from Japan SLC Inc. (Hamamatsu, Japan). Animals were housed under a 12-h light/12-h dark cycle and given free access to food and water. Tumor xenograft models were established by the subcutaneous injection of human pancreatic cancer cells (PANC-1 or MIA PaCa-2, 1×10^7 cells) suspended in 0.1 mL of phosphate-buffered saline and Matrigel (1:1; BD Biosciences, Franklin Lakes, NJ, USA) in nude mice (n = 20). All animal experiments were performed in compliance with the guidelines of the Institute of Experimental Animal Sciences. The protocol was approved by the Animal Care and Use Committee of the Osaka University Graduate School of Medicine. The criteria for euthanasia were as follows: 1) animals shows signs of intolerable suffering, 2) a significant decrease in activity or a marked decrease in food and water intake was observed, 3) the tumor

size reached 3cm in diameter, 4) the observation period ended (after 51 days). Euthanasia was performed by deep anesthesia by isoflurane inhalation.

^{64}Cu-FAPI-04 PET Imaging and Analysis

Tumor xenograft mice (9 weeks old, body weight = 22.5 ± 1.2 g) were investigated using a small animal PET scanner (Siemens Inveon PET/CT) 3 weeks after the implantation of PANC-1 (n = 12) and MIA PaCa-2 (n = 8) when tumor size reached approximately 1.2 cm in diameter (*14*). After the intravenous injection of ^{64}Cu-FAPI-04 (7.21 ± 0.46 MBq), dynamic scans (scan duration = 60 min) were acquired for PANC-1 mice (n = 4) and delayed PET scans (scan duration = 20 min) were acquired 2.5 h after injection for all mice (n = 20) under isoflurane anesthesia. Sinograms were generated in multiple time-frames in the dynamic PET scan (2 min × 30 frames) and in one frame in delayed PET scan. All PET data were reconstructed by two-dimensional ordered-subset expectation maximization (16 subsets, 4 iterations) with attenuation and scatter correction. Regional uptake of

radioactivity was decay-corrected to the injection time and expressed as the standardized uptake value (SUV), which is corrected for the dose (MBq) and body weight (g). Ellipsoid sphere ROIs were manually placed on the tumor, muscle, heart, liver, intestine, kidneys, and bladder of PET images with reference to fused PET/CT. The mean SUV values (SUVmean) were measured to obtain time–activity curves and static uptake in the delayed scan using PMOD (Ver. 3.6).

Comparison of Uptake between ^{64}Cu-FAPI-04 and ^{68}Ga-FAPI-04

Static scans 1 hour after the injection of ^{68}Ga-FAPI-04 (3.6 ± 1.4 MBq) were performed using the same cohort of xenograft mice. Uptake rates were compared between ^{64}Cu-FAPI-04 and ^{68}Ga-FAPI-04 using PANC-1 or MIA PaCa-2 xenograft mice (n = 4 each).

Immunohistochemistry

Immunohistochemical staining was performed to confirm FAP expression in the tumor xenograft using a FAP-alpha antibody. After the animals were sacrificed by

euthanasia, all tumor xenografts were resected and fixed with 4% paraformaldehyde (overnight, 4°C). The fixed tissues were immersed in 30% sucrose in phosphate-buffered saline (overnight, 4°C). Frozen sections of the samples were then incubated with anti-FAP, alpha antibody (ab53066; Abcam, Cambridge, UK). Immunohistochemistry was performed using the Dako EnVision + System - HRP Labelled Polymer Anti-Rabbit (K4003) (DAKO Corp., Glostrup, Denmark). Staining without the primary antibody was also performed to confirm its specificity as a negative control. The stained sections were analyzed by light microscopy (Keyence, Osaka, Japan).

***In Vitro* Cellular Uptake Analysis**

Cellular uptake analysis was performed to confirm that the expression of FAP was not observed in the tumor cell itself but in the stroma of the tumor xenograft. C6 glioma cells were obtained from RIKEN BRC (Tsukuba, Japan) and used as a negative control for the FAP expression test. PANC-1 cells, MIA PaCa-2 cells, and

C6 glioma cells were seeded onto 24-well plates (1×10^5 cells/well) and cultured overnight. ^{64}Cu-FAPI-04 solution (40kBq/250μL) was added to each well and incubated for 10 min. Cells were washed twice with PBS and collected in solutions after they were lysed with 0.1N NaOH. Radioactivity of the collected solution was measured by AccuFlex γ7000 (Hitachi Aloka, Japan). The amounts of proteins were measured in a plate reader (iMark, BIORAD, USA) using the BCA protein assay kit (FUJIFILM Wako Pure Chemical Corporation, Osaka, Japan).

Biodistribution and Treatment Effect of ^{225}Ac-FAPI-04

^{225}Ac-FAPI-04 (10 kBq) was injected into PANC-1 xenograft mice (n = 6, 3 weeks after implantation, tumor size: 814 ± 272 mm^3) to evaluate the whole-body biodistribution. Animals were sacrificed by euthanasia at 3- and 24-h post-injection and samples of major organs were collected after dissection. For the bone and muscle, part of the rear limb was collected. For the collection of bone marrow, 0.8 mL of saline was used for flushing. Radioactivity of each sample was measured

using a 2480 Wizard^2 Gamma Counter (Perkin Elmer, Waltham, MA, USA). Radioactivity counts were normalized by calibration using the ^{225}Ac standard solution. Excrement in the cage was also measured to calculate the excretion rate at 3- and 24-h post-injection. At 3 h post injection, lung data were not available owing to a technical problem. ICR mice (7 weeks old, n = 3) were used as an alternative.

For radioligand therapy using an alpha emitter, ^{225}Ac-FAPI-04 (34 kBq/100 μL) was injected into PANC-1 xenograft mice via the tail vein (n = 6, 3 weeks after implantation, tumor size: 980 ± 659 mm^3). Tumor size was monitored by the elliptical sphere model calculation using the caliper and compared to that of control mice for up to 51 days (n = 6; tumor size at 3 weeks after implantation: 852 ± 587 mm^3). The equivalent dose (Gy) in the dosimetry of ^{225}Ac was estimated according to a previous report (*15*). Residence times were calculated from the tumoral uptakes at 3- and 24-h post-injection, and the area under the curve after 24 h was assumed to decrease with physical decay. Energy per decay (MeV/Bq·s) of ^{225}Ac was estimated

as 28.0 from the alpha particle energy and recoil energy including the emission from all daughter nuclides.

Statistical Analysis

Comparisons between two groups were performed using Mann–Whitney *U* test and SPSS (v.25.0; IBM Corp., Armonk, NY, USA), and a $p < 0.05$ indicated statistical significance.

RESULTS

Dynamic PET images of the ^{64}Cu-FAPI-04 in PANC-1 xenograft model are summarized in Fig. 1. Rapid clearance through the kidneys and slow washout from the tumors were observed (Fig. 2). Delayed PET imaging of ^{64}Cu-FAPI-04 showed moderate uptake in the tumors and relatively high uptake in the liver and intestine (Fig. 3). The SUVmeans of delayed scans were 0.23 ± 0.07 in the PANC-1 xenograft, 0.17 ± 0.03 in the MIA PaCa-2 xenograft,

0.04 ± 0.03 in the muscle, 0.10 ± 0.03 in the heart, 0.91 ± 0.23 in the liver, 0.32 ± 0.17 in the intestine, 0.52 ± 0.48 in the kidneys, and 26.72 ± 31.11 in the bladder (Fig. 4A). Accumulation in the tumor or most of the normal organs was significantly higher for ^{64}Cu-FAPI-04 than for ^{68}Ga-FAPI-04, and excretion in the urine was higher for ^{68}Ga-FAPI-04 than for ^{64}Cu-FAPI-04 (Fig. 3B and Fig. 4C/4D). Immunohistochemical staining revealed abundant FAP expression in the stroma of both PANC-1 and MIA PaCa-2 xenografts (Fig. 5). *In vitro* cellular uptake analysis revealed minimal accumulation in the PANC-1 and MIA PaCa-2 tumor cells (Supplemental Fig.1). The biodistribution of ^{225}Ac-FAPI-04 is shown in Table 1. The liver, kidney, and tumor (PANC-1 xenograft) showed high uptake, although moderate washout from the tumor was observed between 3- and 24-h post-injection. Excrement samples at 24 h were 91.2 ± 13.1 %ID in urine and 2.10 ± 0.10 %ID in feces. ^{225}Ac-FAPI-04 injection showed significant tumor growth suppression in the PANC-1

xenograft mice compared to the control mice, without a significant change in body weight (Fig. 6). The equivalent dose in the tumor was estimated to be 5.68 ± 0.77 Gy/MBq.

DISCUSSION

We evaluated FAP expression in human pancreatic cancer xenografts using ^{64}Cu-FAPI-04 PET with histological confirmation and demonstrated the treatment effect of ^{225}Ac-FAPI-04. We have successfully shown the proof of concept that alpha therapy targeting FAP in the cancer stroma is effective.

FAP has been identified in a wide range of cancer types, such as breast cancer, colon cancer, pancreatic cancer, ovarian cancer, and hepatocellular carcinoma (*11,12*). It shows minimal expression in normal tissues. For targeted alpha therapy, side effects associated with tracer accumulation in normal tissues may present a major issue. For example, side effects in the salivary gland

(xerostomia) have been reported in association with physiological accumulation for targeted alpha therapy using ^{225}Ac-PSMA-617 (*1,16*). Therefore, the low FAP expression in normal tissues is a great advantage for targeted alpha therapy using FAPI. Furthermore, most cancer therapies target markers of tumor cells; alpha therapy targeting FAP is a new treatment option that can be used in combination with other therapies directly targeting cancer cells. Since the microenvironment in cancer is heterogeneous, combinations with other ligands that are internalized in tumor cells are an interesting strategy to irradiate the tumor by alpha particles from both inside and outside of cancer cells.

After the administration of ^{225}Ac-FAPI-04, necrotic collapse of the tumor xenograft, as revealed by a dark brown scab on the skin surface of the xenograft, was observed (Supplemental Fig. 2). We occasionally observed this phenomenon if the tumor size reached a large size in control mice. However, mice treated with ^{225}Ac-FAPI-04 showed collapse at a much smaller tumor size

(1,536 ± 651 mm^3), followed by the shrinkage of the tumor around day 20. Extensive tumor necrosis has also been reported after treatment with molecular targeting drugs (*17,18*). The destruction of the cancer stroma may make it difficult to maintain the structure of the tumor mass due to the alpha irradiation effect of ^{225}Ac-FAPI-04.

Both PANC-1 and MIA PaCa-2 cells are major cell lines of pancreatic ductal adenocarcinoma and that reportedly harbor *KRAS* and *TP53* gene mutations and exhibit neuroendocrine differentiation (*19*). In cellular morphological patterns, PANC-1 cells display a heterogeneous size population, whereas MIA PaCa-2 cells display relatively homogeneous size. Regarding stromal cell composition, human pancreatic cancer samples shows large, solid structures of stroma, whereas xenografts in mice display a relatively scattered stromal distribution (*20*), which is consistent with the present study. Here, we investigated subcutaneously implanted xenograft models rather than those initiated by

intrapancreatic implantation in order to measure tumor size over time using the caliper. Moreover, we used a relatively larger-sized xenograft model, given that smaller tumors showed relatively lower expression of FAP (data not shown).

For the biodistribution of ^{64}Cu-FAPI-04 and ^{225}Ac-FAPI-04, a similar trend was observed in physiological accumulation. It showed high accumulation in the liver and kidney with a large amount of excretion observed in the urine and mild accumulation in the intestine. Rapid excretion through the kidney was also observed for ^{68}Ga-FAPI-04. The increased liver uptake of ^{64}Cu (Fig.4) is most probably due to free radionuclides, because macrocyclic copper-chelates can suffer from limited *in vivo* stability against superoxide dismutase in the liver (*21*). Rylova et al. reported that ^{64}Cu-DOTA-TATE is more stable in humans than in mice (*22*). It is possible that ^{64}Cu- or ^{225}Ac-labeled FAPI-04 shows different biodistribution in humans, especially for liver uptake. Regarding the kinetics of FAPI, relatively rapid wash-out from the tumor is a major problem

during the use of FAPI-04 for radioligand therapy. FAPI compounds, such as FAPI-21 or -46, which exhibit improved tumor retention, should be used in future studies (*10*). Furthermore, for future studies, short-half-life isotopes, such as ^{211}At (7.2 h), would likely be optimal with FAPI; however, FAPI labeling with ^{211}At is currently technically difficult. Here, we only attempted a proof of concept of the effectiveness of targeting FAP in cancer stroma with an alpha emitter.

The injected dose of ^{225}Ac-FAPI-04 in this study was 34 kBq per mouse. Based on body weight, this corresponds to a dose of 1.5 MBq/kg in humans (60 kg). Although this dose is relatively high as compared with ^{225}Ac-PSMA-617 therapy (50–200 kBq/kg), the optimal dose depends on ligand biodistribution and kinetics (*23*). In ^{225}Ac-FAPI-04 therapy, 89% of the injected dose was excreted in the urine at 3-h post-injection due to the rapid kinetics of FAPI, resulting in a low residual amount of the ligand remaining in the body. We did

not acquire later time-point images via ^{64}Cu-FAPI-04 PET (e.g., 24- or 48-h post-injection) due to the limited experimental schedule. However, it is feasible to acquire these images in order to evaluate tracer kinetics and accurately calculate residence time for long-half-life radionuclides (^{64}Cu and ^{225}Ac). We observed no significant change in body weight after the administration of ^{225}Ac-FAPI-04, suggesting that it has minimal toxicity. For a more detailed evaluation of safety, hematological or renal toxicity should be further investigated.

There are some limitations to the present study. We evaluated the treatment effect of a single dose (34 kBq) in only a PANC-1 model, because the supply of ^{225}Ac is very limited in Japan at the moment. Evaluations of dose dependency, optimization, and toxicity are still needed for the clinical application of alpha therapy targeting FAP. We used *in vitro* cellular uptake analysis to confirm that FAP expression was not observed in the tumor cell itself. Although the lack of

a positive control in the assay represents a limitation, it is possible that FAP expression can be observed in the xenograft (*in vivo* situation). FAP staining revealed a brown-stained area around the tumor cells, with some forming streak-like structures suggestive of fibroblasts exhibiting FAP expression. However, clear differentiation between stroma and cytoplasm or specific staining of the stroma is technically challenging work. Confirming the cellular specificity of FAP expression, as well as the effective mechanism of ^{225}Ac-FAPI-04 treatment, requires clarification in future work.

CONCLUSION

This study provided a proof of concept for the use of ^{64}Cu-FAPI-04 and ^{225}Ac-FAPI-04 to treat FAP-expressing pancreatic cancer. Alpha therapy targeting FAP in the cancer stroma is effective and will contribute to the development of a

new treatment strategy in combination with other therapies directly targeting cancer cells.

DISCLOSURE

This study was funded by the KAKENHI (B) (Research Number: 19H03602) from the Ministry of Education, Culture, Sports, Science and Technology (MEXT), and the QiSS program of the OPERA (Grant Number: JPMJOP1721) from the Japan Science and Technology Agency (JST), Japan. There is no other potential conflict of interest relevant to this article to disclose. Patent application for quinoline based FAP-targeting agents for imaging and therapy in nuclear medicine (CK, TL, UH, FLG).

ACKNOWLEDGMENTS

We would like to thank Takanori Kobayashi and Takashi Yoshimura for their excellent technical assistance. $^{229}Th/^{225}Ac$ is provided by the ^{233}U cooperation project between JAEA and the Inter-University Cooperative Research Program of the Institute for Materials Research, Tohoku University (proposal no. 19K0053).

Key Points

Question:

Is the alpha therapy targeting fibroblast activation protein (FAP) in the tumor stroma effective for the treatment of pancreatic cancer?

Pertinent Findings:

This study showed that ^{64}Cu-FAPI-04 and ^{225}Ac-FAPI-04 could be used in theranostics for the treatment of FAP-expressing pancreatic cancer.

^{225}Ac-FAPI-04 administration showed significant tumor growth suppression in the pancreatic cancer xenograft mice.

Implications for Patient Care:

Alpha therapy targeting FAP in the cancer stroma is effective and will contribute to the development of a new treatment strategy.

References

1. Kratochwil C, Bruchertseifer F, Giesel FL, et al. 225Ac-PSMA-617 for PSMA-targeted alpha-radiation therapy of metastatic castration-resistant prostate cancer. *J Nucl Med.* 2016;57:1941-1944.

2. Giesel FL, Knorr K, Spohn F, et al. Detection efficacy of (18)F-PSMA-1007 PET/CT in 251 patients with biochemical recurrence of prostate cancer after radical prostatectomy. *J Nucl Med.* 2019;60:362-368.

3. Xing F, Saidou J, Watabe K. Cancer associated fibroblasts (CAFs) in tumor microenvironment. *Front Biosci (Landmark Ed).* 2010;15:166-179.

4. Werb Z, Lu P. The role of stroma in tumor development. *Cancer J.* 2015;21:250-253.

5. Tao L, Huang G, Song H, Chen Y, Chen L. Cancer associated fibroblasts: An essential role in the tumor microenvironment. *Oncol Lett.* 2017;14:2611-2620.

6. Zi F, He J, He D, Li Y, Yang L, Cai Z. Fibroblast activation protein alpha in tumor microenvironment: recent progression and implications (review). *Mol Med Rep.* 2015;11:3203-3211.

7. Liu F, Qi L, Liu B, et al. Fibroblast activation protein overexpression and clinical implications in solid tumors: a meta-analysis. *PLoS One.* 2015;10:e0116683.

8. Loktev A, Lindner T, Mier W, et al. A new method for tumor imaging by targeting cancer associated fibroblasts. *J Nucl Med.* 2018 2018;59:1423-1429

9. Lindner T, Loktev A, Altmann A, et al. Development of quinoline-based theranostic ligands for the targeting of fibroblast activation protein. *J Nucl Med.* 2018;59:1415-1422.

10. Loktev A, Lindner T, Burger EM, et al. Development of novel FAP-targeted radiotracers with improved tumor retention. *J Nucl Med.* 2019 [Epub ahead of print].

11. Giesel FL, Kratochwil C, Lindner T, et al. (68)Ga-FAPI PET/CT: Biodistribution and preliminary dosimetry estimate of 2 DOTA-containing FAP-targeting agents in patients with various cancers. *J Nucl Med.* 2019;60:386-392.

12. Kratochwil C, Flechsig P, Lindner T, et al. (68)Ga-FAPI PET/CT: Tracer uptake in 28 different kinds of cancer. *J Nucl Med.* 2019;60:801-805.

13. Apostolidis C, Molinet R, Rasmussen G, Morgenstern A. Production of Ac-225 from Th-229 for targeted alpha therapy. *Anal Chem.* 2015;77:6288-6291.

14. Bao Q, Newport D, Chen M, Stout DB, Chatziioannou AF. Performance evaluation of the inveon dedicated PET preclinical tomograph based on the NEMA NU-4 standards. *J Nucl Med.* 2009;50:401-408.

15. Spetz J, Rudqvist N, Forssell-Aronsson E. Biodistribution and dosimetry of free 211At, 125I- and 131I- in rats. *Cancer Biother Radiopharm.* 2013;28:657-664.

16. Sathekge M, Bruchertseifer F, Vorster M, et al. Predictors of overall and disease free survival in metastatic castration-resistant prostate cancer patients receiving (225)Ac-PSMA-617 radioligand therapy. *J Nucl Med.* 2019 [Epub ahead of print].

17. Blakey DC, Westwood FR, Walker M, et al. Antitumor activity of the novel vascular targeting agent ZD6126 in a panel of tumor models. *Clin Cancer Res.* 2002;8:1974-1983.

18. Beloueche-Babari M, Jamin Y, Arunan V, et al. Acute tumour response to the MEK1/2 inhibitor selumetinib (AZD6244, ARRY-142886) evaluated by non-invasive diffusion-weighted MRI. *Br J Cancer.* 2013;109:1562-1569.

19. Gradiz R, Silva HC, Carvalho L, Botelho MF, Mota-Pinto A. MIA PaCa-2 and PANC-1 - pancreas ductal adenocarcinoma cell lines with neuroendocrine differentiation and somatostatin receptors. *Sci Rep.* 2016;6:21648.

20. Lee HO, Mullins SR, Franco-Barraza J, Valianou M, Cukierman E, Cheng JD. FAP-overexpressing fibroblasts produce an extracellular matrix that enhances invasive velocity and directionality of pancreatic cancer cells. *BMC Cancer.* 2011;11:245.

21. Bass LA, Wang M, Welch MJ, Anderson CJ. In vivo transchelation of copper-64 from TETA-octreotide to superoxide dismutase in rat liver. *Bioconjug Chem.* 2000;11:527-532.

22. Rylova SN, Stoykow C, Del Pozzo L, et al. The somatostatin receptor 2 antagonist 64Cu-NODAGA-JR11 outperforms 64Cu-DOTA-TATE in a mouse xenograft model. *PLoS One.* 2018;13:e0195802.

23. Kratochwil C, Bruchertseifer F, Rathke H, et al. Targeted alpha-therapy of metastatic castration-resistant prostate cancer with (225)Ac-PSMA-617: dosimetry estimate and empiric dose finding. *J Nucl Med.* 2017;58:1624-1631.

	%ID		%ID/g	
	3 h	24 h	3 h	24 h
Brain	0.015 ± 0.004	0.004 ± 0.001	0.047 ± 0.007	0.015 ± 0.004
Submandibular gland	0.034 ± 0.004	0.010 ± 0.001	0.282 ± 0.059	0.083 ± 0.020
Heart	0.031 ± 0.005	0.001 ± 0.003	0.277 ± 0.041	0.013 ± 0.030
Lung	0.028 ± 0.008	0.008 ± 0.005	0.128 ± 0.032	0.041 ± 0.023
Liver	0.745 ± 0.005	0.443 ± 0.032	0.685 ± 0.042	0.374 ± 0.037
Stomach	0.028 ± 0.007	0.009 ± 0.004	0.224 ± 0.060	0.096 ± 0.042
Small intestine	0.229 ± 0.036	0.048 ± 0.008	0.275 ± 0.050	0.055 ± 0.003
Large intestine	0.025 ± 0.005	0.014 ± 0.003	0.434 ± 0.108	0.098 ± 0.019
Kidney	1.117 ± 0.133	0.312 ± 0.022	3.274 ± 0.565	0.883 ± 0.106
Adrenal gland	0.025 ± 0.004	0.005 ± 0.002	1.492 ± 0.186	0.323 ± 0.077
Pancreas	0.029 ± 0.001	0.017 ± 0.008	0.310 ± 0.012	0.140 ± 0.068
Spleen	0.029 ± 0.004	0.018 ± 0.002	0.203 ± 0.006	0.106 ± 0.020
Testis	0.014 ± 0.001	0.007 ± 0.001	0.079 ± 0.008	0.034 ± 0.003
Urine	2.816 ± 2.775	0.073 ± 0.060	40.66 ± 40.25	1.343 ± 0.439
Blood	0.051 ± 0.008	0.024 ± 0.011	0.102 ± 0.021	0.041 ± 0.017
Bone	0.052 ± 0.004	0.027 ± 0.003	0.161 ± 0.007	0.085 ± 0.009
Bone marrow	0.011 ± 0.003	0.003 ± 0.005	0.175 ± 0.082	0.025 ± 0.042
Muscle	0.051 ± 0.011	0.027 ± 0.004	0.061 ± 0.008	0.030 ± 0.001
Tumor	0.173 ± 0.029	0.092 ± 0.023	0.251 ± 0.010	0.097 ± 0.008
Excrement (urine)	88.87 ± 2.81	91.23 ± 13.05	N/A	N/A
Excrement (feces)	N/A	2.102 ± 0.101	N/A	N/A

TABLE 1. Whole-body distribution after the intravenous administration of ^{225}Ac-FAPI-04 in the PANC-1 xenograft model (n = 6). Data are expressed as mean values with standard error (SE). (N/A: not available)

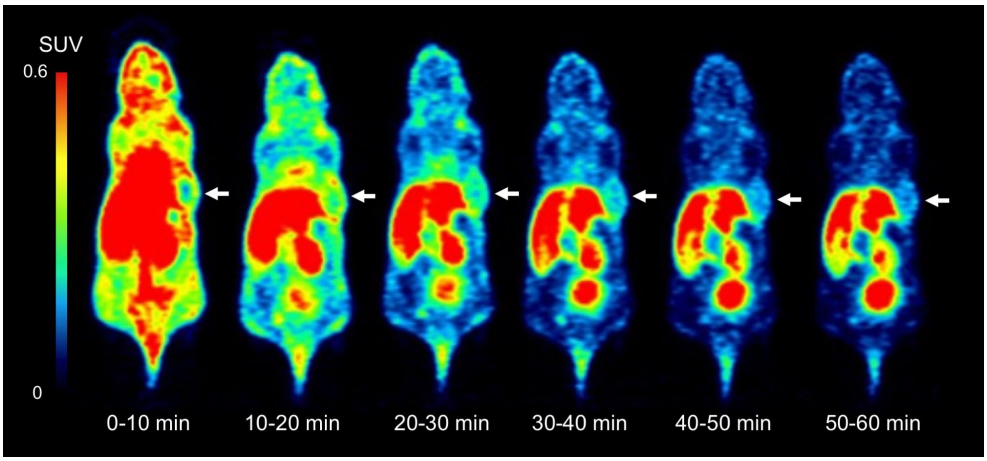

FIGURE 1. Dynamic PET imaging of ^{64}Cu-FAPI-04 in the PANC-1 xenograft model (arrows indicate the tumor xenograft).

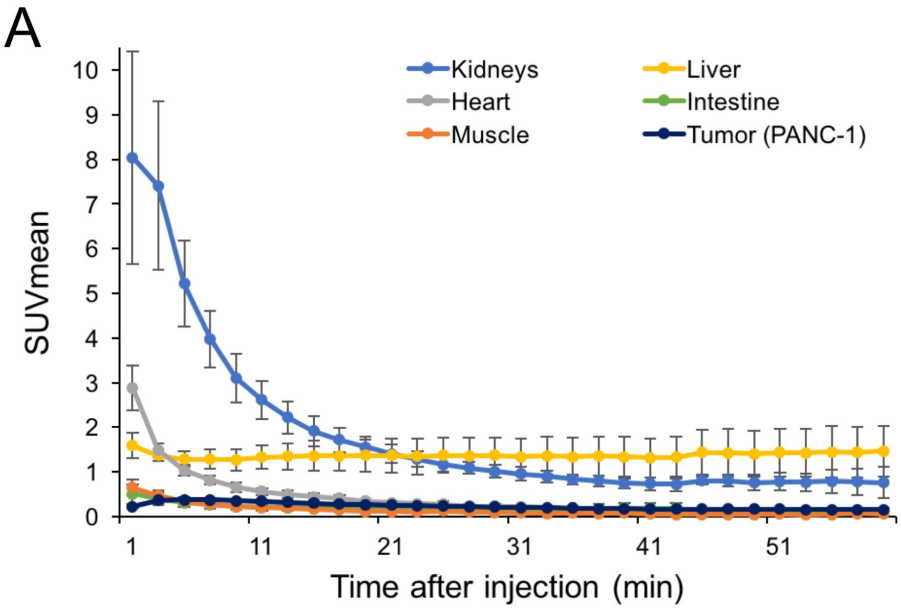
A
Kidneys
Liver
Heart
Intestine
Muscle
Tumor (PANC-1)
SUVmean
Time after injection (min)

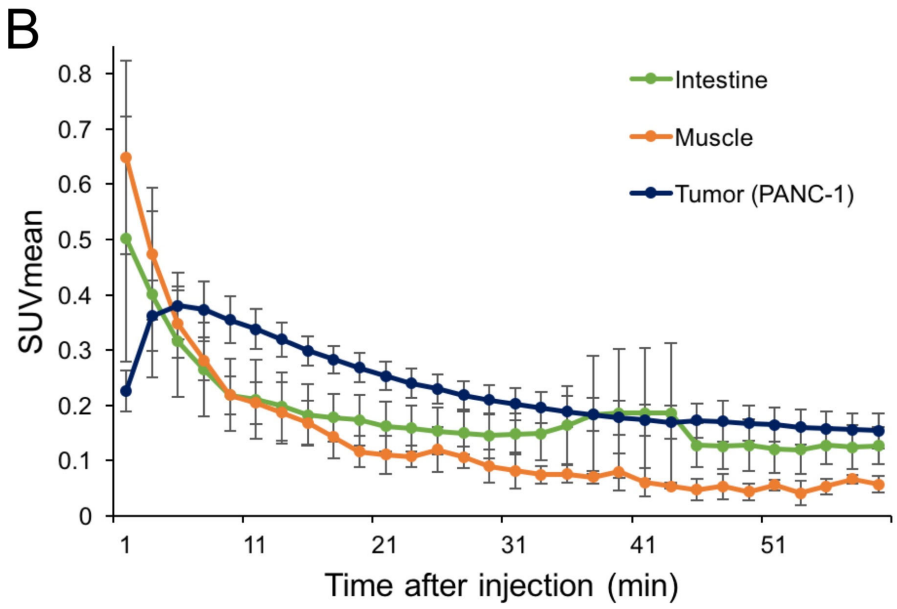
B
Intestine
Muscle
Tumor (PANC-1)
SUVmean
Time after injection (min)

FIGURE 2. Time–activity curve for the PANC-1 tumor and normal organs on ^{64}Cu-FAPI-04 PET. (Note that the vertical scales in the upper and lower panels are different.)

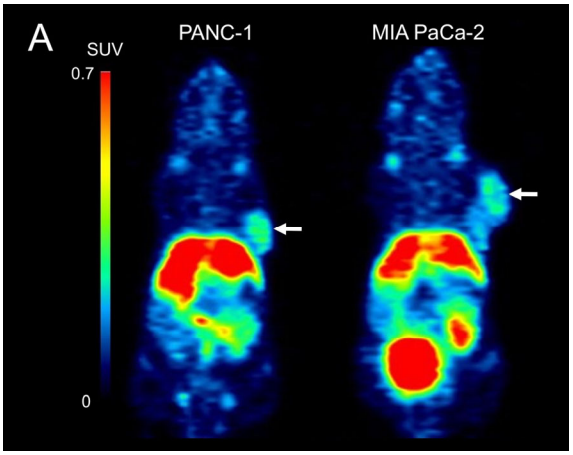
A
SUV
0.7
0
PANC-1
MIA PaCa-2

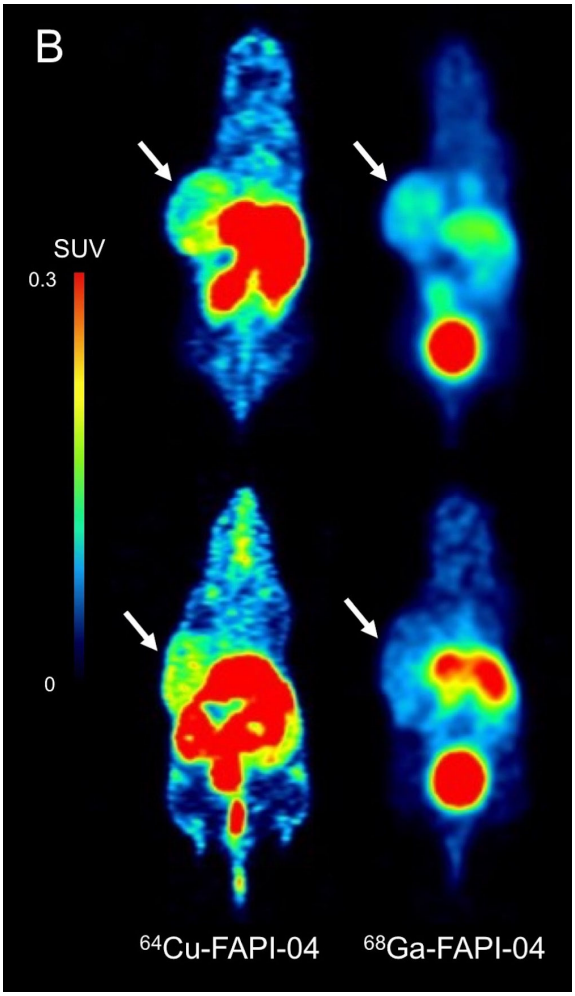
B
SUV
0.3
0
64Cu-FAPI-04
68Ga-FAPI-04

FIGURE 3. (A) Delayed PET imaging of ^{64}Cu-FAPI-04 (2.5-h post-injection) in PANC-1 and MIA PaCa-2 xenograft models. (B) Comparison of uptake rates between ^{64}Cu-FAPI-04 (2.5-h post-injection) and ^{68}Ga-FAPI-04 (1-h post-injection) (Upper: PANC-1 and lower: MIA PaCa-2).

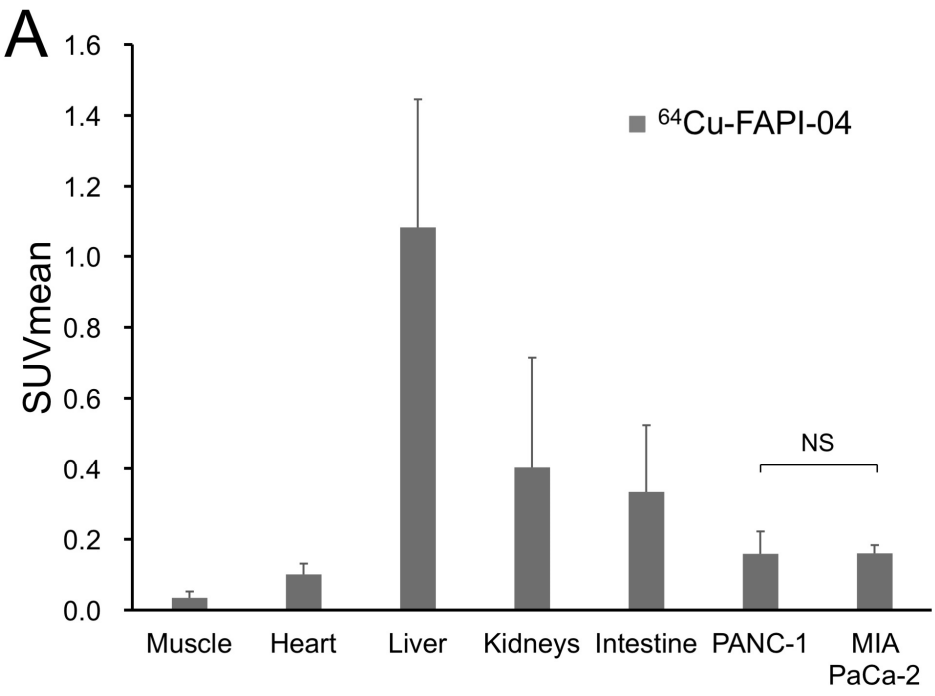
A
SUVmean
1.6
1.4
1.2
1.0
0.8
0.6
0.4
0.2
0.0
64Cu-FAPI-04
NS
Muscle
Heart
Liver
Kidneys
Intestine
PANC-1
MIA PaCa-2

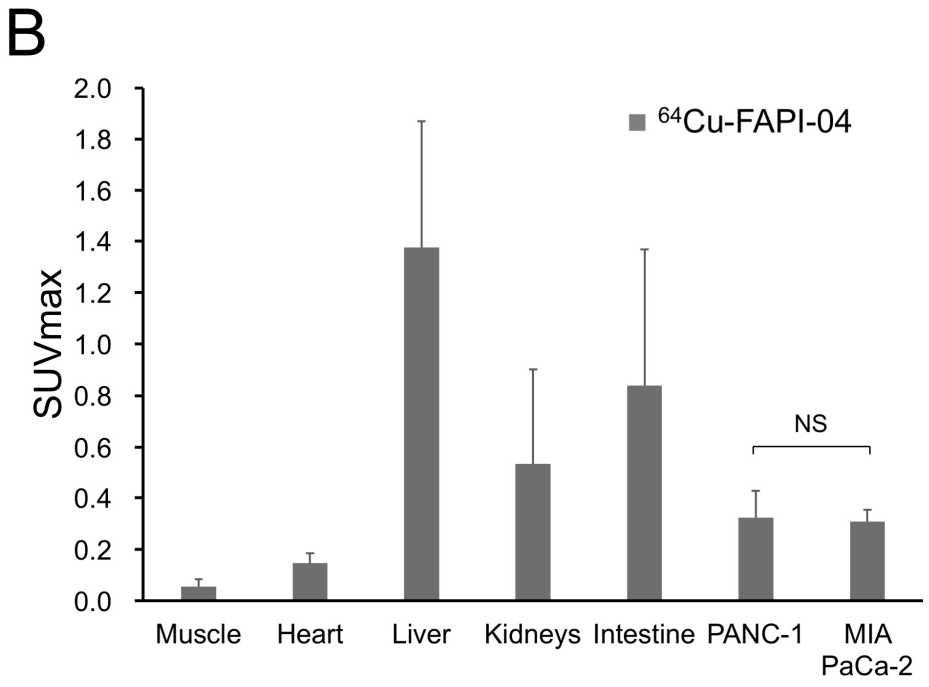
B
SUVmax
2.0
1.8
1.6
1.4
1.2
1.0
0.8
0.6
0.4
0.2
0.0
64Cu-FAPI-04
NS
Muscle
Heart
Liver
Kidneys
Intestine
PANC-1
MIA PaCa-2

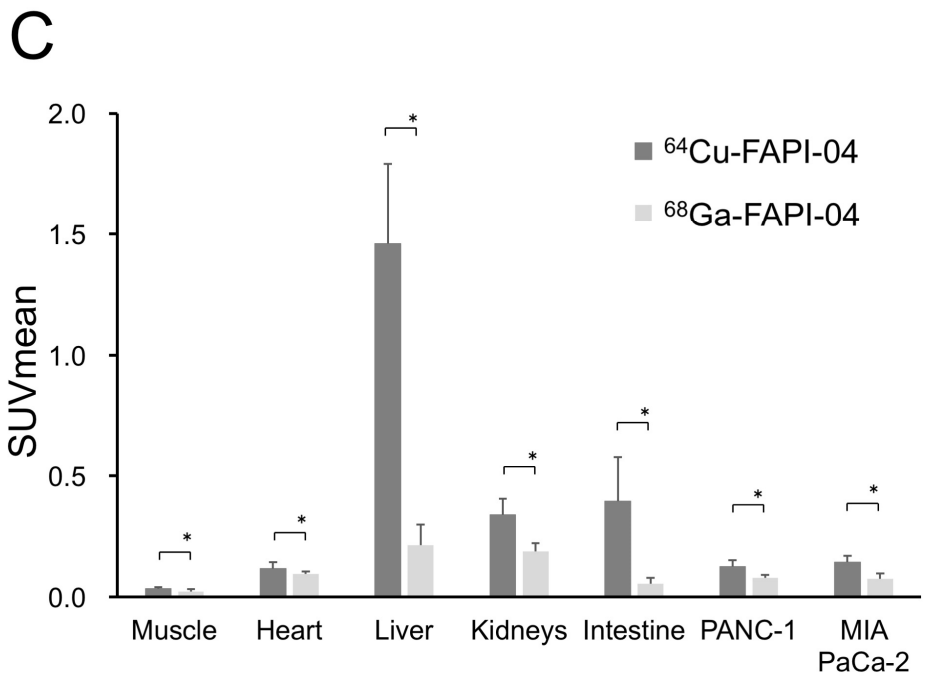
C
SUVmean
2.0
1.5
1.0
0.5
0.0
64Cu-FAPI-04
68Ga-FAPI-04
*
Muscle
Heart
Liver
Kidneys
Intestine
PANC-1
MIA PaCa-2

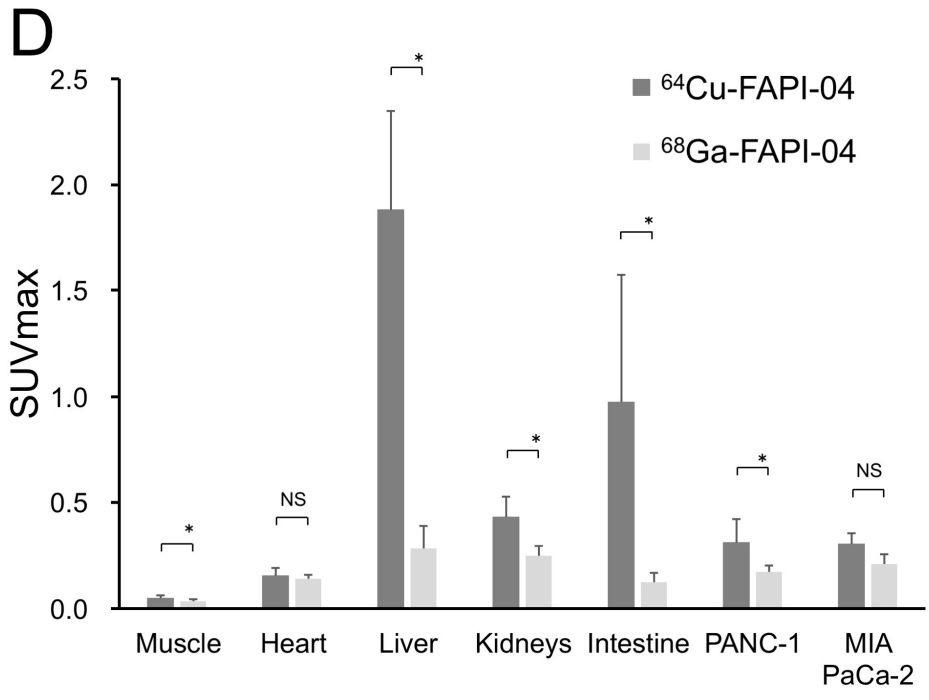
D
SUVmax
2.5
2.0
1.5
1.0
0.5
0.0
64Cu-FAPI-04
68Ga-FAPI-04
*
NS
Muscle
Heart
Liver
Kidneys
Intestine
PANC-1
MIA PaCa-2

FIGURE 4. (A,B) Tracer uptake in the tumor and normal organs on ^{64}Cu-FAPI-04 PET (2.5-h post-injection). (C,D) Comparison of uptake rates in the tumor and normal organs between ^{64}Cu-FAPI-04 and ^{68}Ga-FAPI-04 PET. (*$p < 0.05$, NS: not significant)

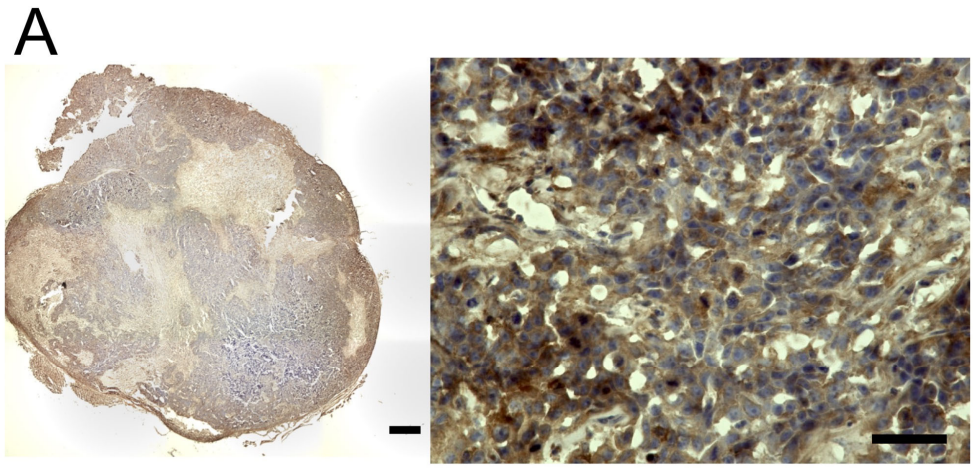
A

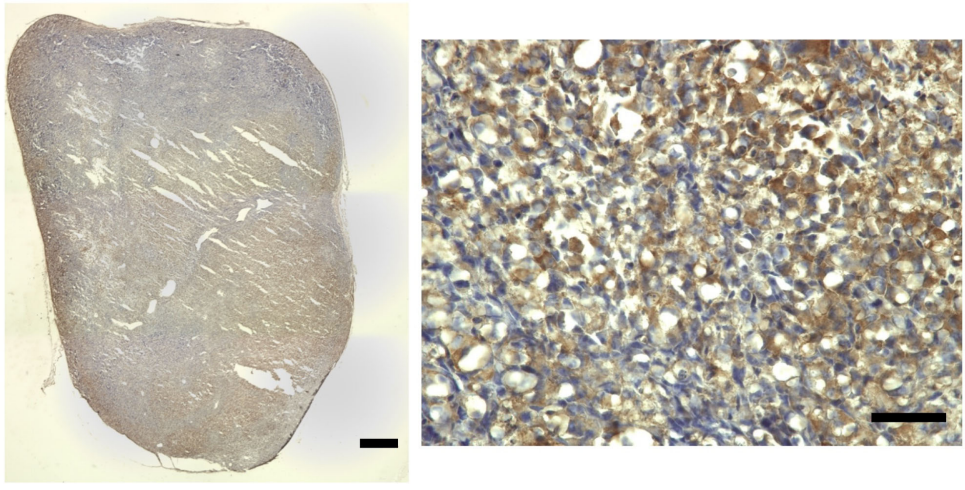
B

C

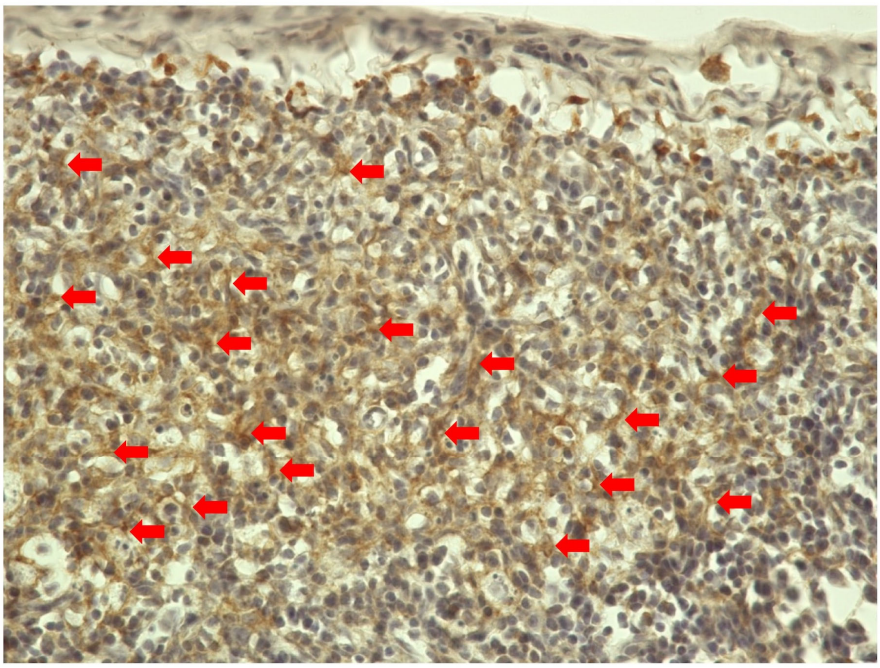

D

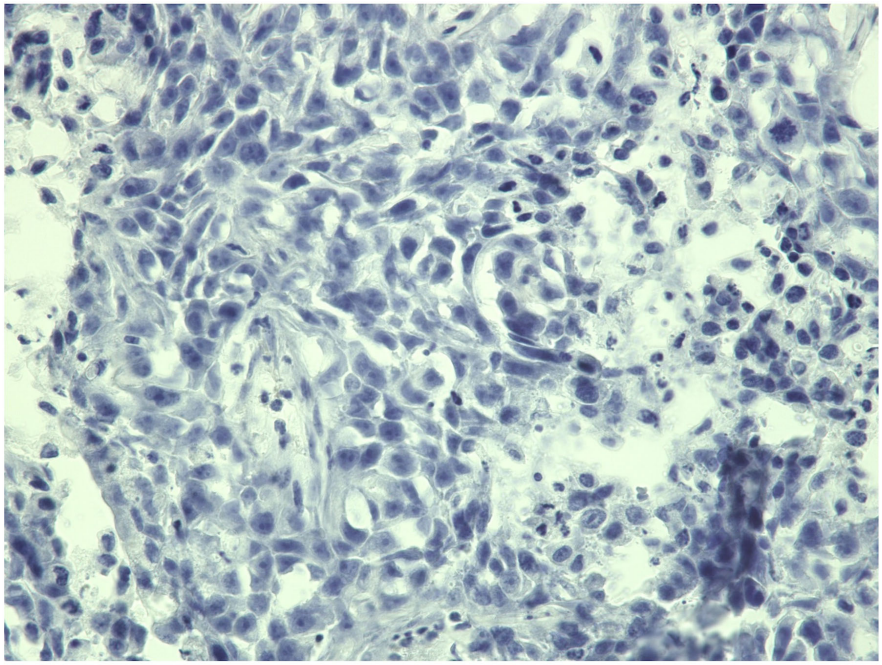

FIGURE 5. Immunohistochemical staining of the (A) PANC-1 and (B) MIA PaCa-2 tumor xenografts using an FAP-alpha antibody (left: low magnification, right: high magnification). The black bar indicates 1000 μm in the left panel and 50 μm in the right panel. (C) Positive-control staining of FAP in the stroma of the PANC-1 xenograft (red arrows indicated stroma) and (D) negative-control staining in the PANC-1 xenograft without the primary antibody (high magnification).

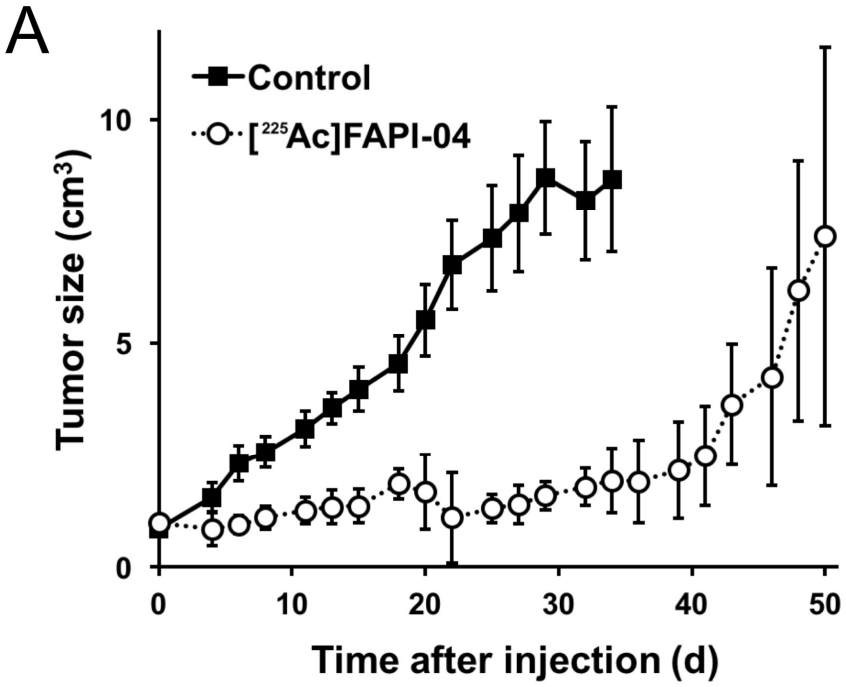
A
Control
[225Ac]FAPI-04
Tumor size (cm3)
0
5
10
0
10
20
30
40
50
Time after injection (d)

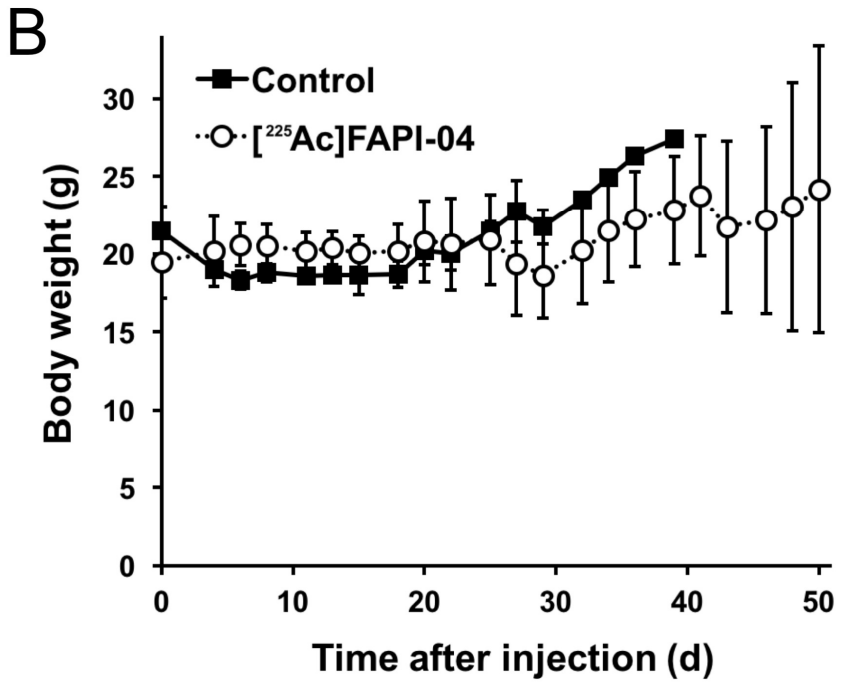
B
Control
[225Ac]FAPI-04
Body weight (g)
0
5
10
15
20
25
30
0
10
20
30
40
50
Time after injection (d)

FIGURE 6. (A) Treatment effect and (B) change in body weight in PANC-1 xenograft mice after the injection of ^{225}Ac-FAPI-04.

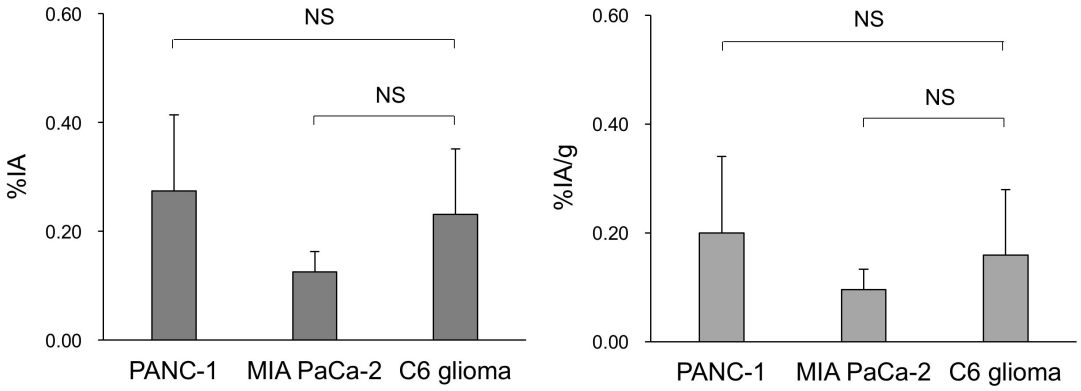

Supplemental Figure 1. *In vitro* cellular uptake assay of ^{64}Cu-FAPI-04 using PANC-1, MIA PaCa-2, and C6 glioma cells for comparison. We observed minimal accumulation in PANC-1 and MIA PaCa-2 cells, with this comparable to that in C6 glioma cells (negative control). Data represent the mean (±SE), percent injected activity (%IA), and percent injected activity per gram (%IA/g).

NS: not significant according to Mann–Whitney *U* test.

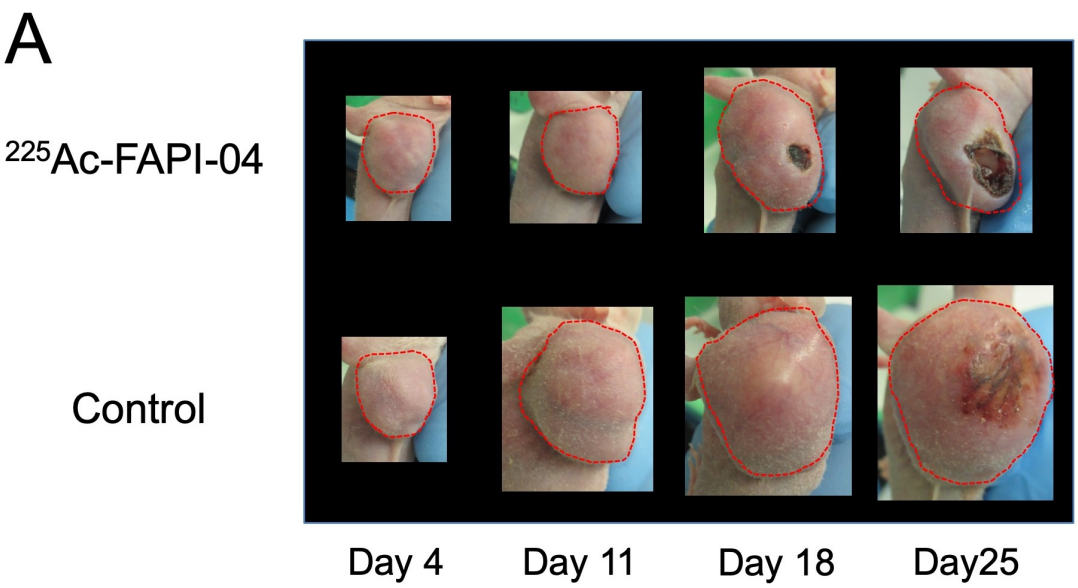

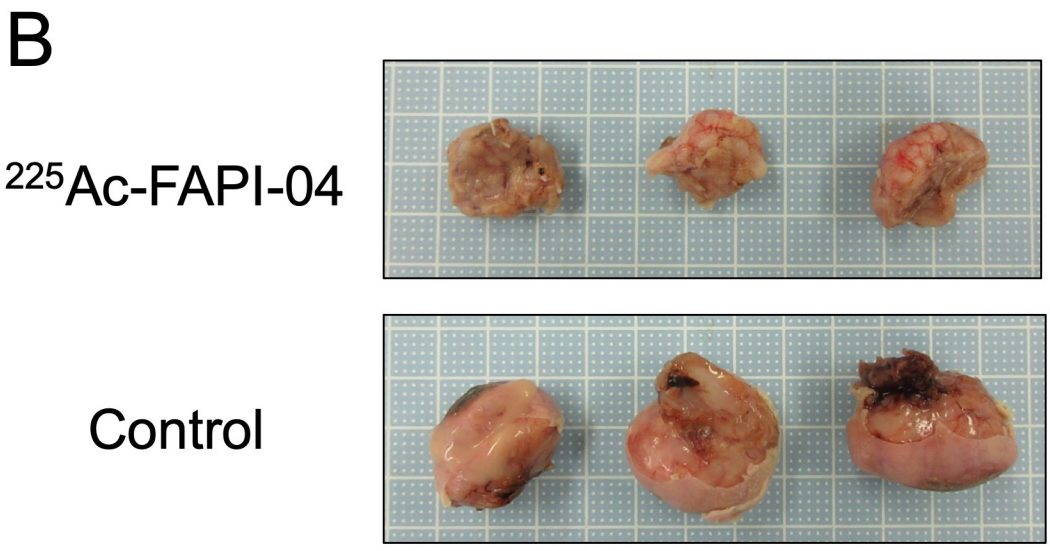

Supplemental Figure 2. (A) Appearance of the xenografts after injection of ^{225}Ac-FAPI-04 and control. A dark-brown scab was observed on the surface of the xenograft at day 18 and

accompanied by mild tumor shrinkage in mice injected with ^{225}Ac-FAPI-04. (B) Tumor appearance after resection at day 31 (2nd cohort), with tumor size smaller in ^{225}Ac-FAPI-04-injected mice relative to that observed in control mice.